separations

MDPI

Article

Application of the Biomass of Leaves of *Diospyros kaki* L.f. (Ebenaceae) in the Removal of Metal Ions from Aqueous Media

Rodrigo Martorelli Galera [1], Adrielli Cristina Peres da Silva [1], Alexandre de Oliveira Jorgetto [2], Marcos Henrique Pereira Wondracek [3], Margarida Juri Saeki [1], José Fabián Schneider [4], Valber de Albuquerque Pedrosa [1], Marco Autônio Utrera Martines [5] and Gustavo Rocha Castro [1,*]

1 Chemistry and Biochemistry Department, Institute of Biosciences of Botucatu-UNESP, C.P. 510, Botucatu 18618-000, SP, Brazil; rmgallera@yahoo.com.br (R.M.G.); adrielli.peres@unesp.br (A.C.P.d.S.); mjsaeki@unesp.br (M.J.S.); valber.pedrosa@unesp.br (V.d.A.P.)
2 Interdisciplinary Laboratory of Nanostructures and Semiconductors (LINSE-IQ-UNESP), Rua Francisco Degni, 55, Araraquara 14800-060, SP, Brazil; xjorgetto@gmail.com
3 Faculty of Science and Technology, University of Grande Dourados, Rodovia Dourados-Itahum, km 12, Dourados 79804-970, MS, Brazil; marcoswondracek@gmail.com
4 Instituto de Física, Universidade de São Paulo (USP), São Carlos 13566-590, SP, Brazil; schnei@ifsc.usp.br
5 Institute of Chemistry, INQUI—Federal University of Mato Grosso do Sul, Campo Grande 79074-460, MS, Brazil; marcomartines@gmail.com
* Correspondence: castrogr@ibb.unesp.br; Tel.: +55-014-38800578

Abstract: Using straightforward and cost-effective methods, persimmon leaves were converted into high-quality powder. This powder was applied as an adsorbent for the removal of Cu(II) and Cd(II) from aqueous solutions. Scanning electron microscopy (SEM) revealed the presence of particles with non-homogeneous sizes and rough textures. The biosorbent exhibited a specific surface area of approximately 0.44 ± 0.015 m^2 g^{-1}. Elemental analysis and energy-dispersive X-ray spectroscopy (EDX) confirmed the presence of elements such as sulfur, phosphorus, nitrogen, and oxygen. The results of ^{13}C nuclear magnetic resonance (^{13}C-NMR), obtained using the cross-polarization technique, show the presence of groups containing sulfur and oxygen. Infrared spectroscopy (FTIR) indicated the existence of amine and hydroxyl groups. The material was used in the solid-phase extraction of Cu(II) and Cd(II) in batch experiments, and its adsorption capacity was evaluated as a function of time, pH, and analyte concentration. The fraction with a diameter between 63 and 106 µm was selected for the adsorption tests. Kinetic equilibrium was reached within 5 min, and the experimental data were fitted to the pseudo-second-order kinetic model. The optimum pH for the adsorption of both metal species was approximately 5.0. The adsorption isotherms were adjusted using the modified Langmuir equation, and the maximum amount of metal species extracted from the solution was determined to be 0.213 mmol g^{-1} for Cu(II) and 0.215 mmol g^{-1} for Cd(II), with high linear correlation coefficients for both metals. Persimmon leaves are typically abundant during the growing season, and because they are seasonal, the *Diospyros kaki* L.f. tree undergoes the natural process of leaf abscission, ensuring the availability of leaves for application.

Keywords: adsorption; heavy metals; persimmon leaves; copper ions; cadmium ions; aqueous solutions; solid-phase extraction

check for updates

Citation: Galera, R.M.; da Silva, A.C.P.; Jorgetto, A.d.O.; Wondracek, M.H.P.; Saeki, M.J.; Schneider, J.F.; Pedrosa, V.d.A.; Martines, M.A.U.; Castro, G.R. Application of the Biomass of Leaves of *Diospyros kaki* L.f. (Ebenaceae) in the Removal of Metal Ions from Aqueous Media. *Separations* **2024**, *11*, 12. https://doi.org/10.3390/separations11010012

Academic Editor: Hideo Maruyama

Received: 31 August 2023
Revised: 25 October 2023
Accepted: 26 October 2023
Published: 27 December 2023

Copyright: © 2023 by the authors. Licensee MDPI, Basel, Switzerland. This article is an open access article distributed under the terms and conditions of the Creative Commons Attribution (CC BY) license (https://creativecommons.org/licenses/by/4.0/).

1. Introduction

The persistent rise in environmental contamination due to noxious agents such as pesticides, dyes, pharmaceutical products, and potentially harmful metal species is an alarming trend. This phenomenon can be ascribed to the heightened industrial and agricultural activities aimed at fulfilling the growing demands of the population, the indiscriminate use of fossil fuels, and the exploitation of mineral resources. Consequently, the adverse repercussions of these detrimental anthropogenic practices are increasingly evident in

the environmental impact of effluents containing toxic substances. The non-sustainability of production and exploitation methods is primarily responsible for contamination [1–3] (CARNEIRO et al., 2010; MINELLO et al., 2009; GARCÍA- SÁNCHEZ et al., 2022). Among the various types of environmental pollutants, potentially toxic metal species (formerly known as heavy metals) are responsible for several deleterious effects on organisms [4–6]. After entering the environment, heavy metals such as copper, cadmium, zinc, lead, chromium, and arsenic can spread through the lithosphere, hydrosphere, and atmosphere, causing contamination across a significant portion of the planet. One of the most common ways of dispersion is through water, as they become solubilized in liquid media and then discharged into bodies of water that carry them over long distances from their sources, or by infiltration into the ground, reaching the groundwater. They can also be dispersed in the atmosphere, becoming adsorbed onto solid particles resulting from the burning of materials containing such elements. In this case, they can deposit on soils, lakes, and rivers, reaching distant regions, or undergo precipitation along with rain, causing contamination of large areas [7,8]. As environmental pollutants, potentially toxic metal species do not undergo degradation and can be converted into organometallic species by bacterial activity in the medium. These compounds interact with organisms and are introduced into the food chain, causing the bioaccumulation and biomagnification of heavy metals in the environment [6,7,9]. Organometallic compounds tend to pose a higher level of harm than free metal cations. This elevated hazard stems from their heightened attraction to the fatty tissues of aquatic organisms, leading to significantly higher bioconcentration factors. Consequently, we can observe intoxication in communities that depend on aquatic animals for food [6,7,9]. Given the inherent risks associated with the contamination of drinking water by heavy metals, which has a direct impact on human health, it is of great importance to develop and apply techniques for wastewater remediation. These techniques prevent the emission of toxic metal species and the contamination of rivers, lakes, and seas. Among the methods for removing metal species from aqueous samples, solid-phase extraction using adsorbent materials is widely used because of its low cost, simplicity, and the possibility of anchoring different molecular ligands on the surfaces of the materials [10–20]. This technique takes advantage of the presence of chelating or complexing groups (such as amines, amides, carboxylic acids, and hydroxyls) on the surface of the adsorbent, which are capable of sequestering metal ions and allowing the removal of such species from aqueous solutions. The chemical process entails the creation of covalent coordinate bonds between metal cations, which act as Lewis acids, and chemical molecules or groups anchored to the adsorbent surface, which act as Lewis bases. Lewis bases, including organic groups containing elements such as N, O, S, and P, possess unshared electrons that can form covalent bonds with electron-deficient species (in this scenario, the metal cations). This ensures the secure immobilization of the metal species on the adsorbent, facilitating their effective removal [21]. Over time, several adsorbents have been proposed for remediating metal-contaminated wastewater, such as modified silicas, activated carbon, zeolites, sand, clays, cellulose polymers, and industrial and agricultural residues [22–29]. Nevertheless, certain materials require an organic functionalization process to enhance their adsorption capacity prior to their use as adsorbents. During this stage, a complexing or chelating molecule is bonded to the material surface, enabling it to effectively extract metal ions from the solution [18,20,27,30]. Organofunctionalized materials present a serious disadvantage in terms of their application, namely, the use of expensive reagents and solvents, as well as the generation of toxic waste during their synthesis and functionalization, which makes large-scale production for environmental purposes impractical [16,18,20,30]. As an eco-friendly substitute for synthetic materials, a range of adsorbents can be created from abundant naturally occurring organic materials, making them suitable for use in solid-phase extraction methods. Biomaterials, in particular, possess inherent complexing groups within their chemical composition, obviating the necessity for additional functionalization processes. The adsorption capabilities of these natural materials are linked to the inclusion of N, O, P, and S atoms (which act as Lewis bases) in their complexing groups, enabling the

formation of covalent bonds through electron pair sharing with the metal species present in the solution [31,32].

These biomaterials can be readily gathered and undergo uncomplicated preparation using basic techniques such as drying, milling, and sieving, enabling their transformation into a finely powdered form suitable for conducting solid-phase extraction of metal species from aqueous solutions [33,34]. Biomaterials have emerged as a compelling and cost-effective option for producing adsorbents to remediate wastewater [21,35]. Several biomaterials, such as banana peels [31], castor leaves [32], cassava root husks [35], sugarcane bagasse [36], orange peels [37], peanut shells [38], coconut fibers [39], pine bark [40], grass biomass [41], rice husk ash [42], green coconut shells [43], and corn leaves [44] have already been studied regarding their adsorption capacities, demonstrating their effective removal of metal species from aqueous solutions. In addition to their low cost and ease of preparation, some of these materials can be reused for several adsorption/desorption cycles [31,32,45]. To gauge a material's potential suitability as an adsorbent, it is crucial to delve into the fundamental facets of its physicochemical properties. This inquiry aids in determining the attraction between the adsorbent and specific metal species, along with understanding the impact of environmental conditions such as pH and contact time on the material adsorption capacity. In this study, we assessed the viability of a powder derived from *Diospyros kaki* L.f. (persimmon) leaves as a promising biosorbent for the removal of Cu(II) and Cd(II) from aqueous samples. The choice of this material is based on sustainability, as the leaves of this tree naturally fall during a certain period of the year (when the tree enters a stage of senescence), generating a large amount of available biomass [46]. Biosorbents, in addition to originating from renewable sources, have become a promising material as they do not require chemical modifications, making them even more economically viable [47–49]. Thus, several relevant parameters that influence the adsorption process of metal species were investigated to elucidate the biosorbent properties of persimmon leaves.

2. Materials and Methods

2.1. Solvents, Solutions, and Reagents

Solutions of Cu(II) and Cd(II) were prepared by dissolving their respective high-purity chlorides (Sigma-Aldrich, Steinheim, Germany) in ultrapure deionized water (18.2 MΩ·cm^{-1}, Direct-Q system, Millipore, France) to obtain stock solutions of approximately 500 mg L^{-1} for both metals. Treatments involving Cu(II) and Cd(II) solutions of distinct concentrations were prepared by dilution, starting from the stock solutions, to achieve the intended concentrations. Standard metal solutions used for calibration of the spectrometer were prepared by diluting their respective 1000 mg L^{-1} stock solutions (Specsol, Brazil). For pH adjustment, dilute solutions of HNO_3 (Carlo Erba), and NaOH (Merck, Darmstadt, Germany) were used. All containers were washed with 10% v.v. HNO_3 for at least 24 h, rinsed with deionized water, and dried at room temperature or in an oven heated to 50 °C before use.

2.2. Preparation of the Biosorbent

Persimmon leaves were collected in the city of Botucatu, Brazil, and thoroughly washed with ultrapure water. They were placed in paper bags and stored in a ventilated chamber heated to 100 °C for one week to ensure complete drying. The dried material was manually ground and processed in a knife mill, resulting in a crude powder with particles of varying sizes. Subsequently, the material was sieved using sieves with different pore diameters. The fraction with a diameter between 63 and 106 µm was selected for the adsorption tests. Before conducting the experiments, the material underwent a washing process in a Soxhlet system using 500 mL of distilled water, until the washing effluent achieved clarity. This procedure was performed with the objective of eliminating water-soluble organic compounds liberated from the powder, which might otherwise interact with the metal ions and potentially hinder their adsorption onto the persimmon leaf particles.

The washed material was subsequently transferred to a heated oven set at 55 °C to facilitate the evaporation of any residual solvent.

2.3. Equipment

The material was characterized by Fourier transform infrared spectroscopy (FTIR) using a Nicolet Nexus 670 spectrometer (Thermo, EUA, Waltham, MA, USA). The sample was scanned 200 times with a resolution of 4 cm^{-1} in transmittance mode. A 200 mg KBr pellet containing 1% by weight of the sample was prepared to collect the spectrum of the persimmon leaves. Nitrogen, hydrogen, and carbon contents were determined through elemental analysis of 2.0 mg persimmon leaf powder using a Thermo Finnigan Flash 1112 Series EA CHNS elemental analyzer (CE Instruments, Wigan, UK). The concentrations of Cu(II) and Cd(II) were obtained at their most sensitive resonance spectral lines (324.7 and 228.8 nm, respectively) using a Shimadzu AA 7000 atomic absorption spectrometer in flame atomization mode (air–acetylene mixture). The morphology of the particles was observed using a Quanta 200 scanning electron microscope (FEI Company, Quezon City, Philippines), and the surface areas of the investigated materials were determined according to the BET (Brunauer–Emmett–Teller) model. Elemental mapping of N, P, S, and O was performed using an X-Max accessory (Oxford equipment) coupled to the electron microscope. The sample particles were dispersed in isopropanol, and the suspension was poured onto a glass slide. After drying, the sample was coated with gold. High-resolution ^{13}C-NMR experiments were conducted under a magnetic field of 5.9 T using a DD2 NMR Agilent spectrometer. Samples were spun at up to 5.0 KHz in 4 mm zirconium rotors under magic angle conditions. The ^{13}C spectra were obtained from {^{1}H}-^{13}C cross-polarization experiments by applying a $\pi/2$ pulse of 6.0 μs on ^{1}H, a contact time of 1.0 ms, and a recycle delay of 5.0 s. 20,000 signals were collected. High-power proton decoupling was applied during the acquisition period in the cross-polarization experiments. A solid adamantine sample was used as a secondary standard for ^{13}C isotropic chemical shift (high-frequency resonance at 38.6 ppm relative to tetramethylsilane, TMS) and for calibration of the {^{1}H}-^{13}C cross-polarization conditions.

2.4. Point of Zero Charge (pH_{PZC})

To provide a more comprehensive characterization of the adsorbent surface, we determined the point of zero charge (pH_{PZC}) using the immersion method. In these experiments, 25.0 mg of the powdered material was transferred to several Falcon tubes and stirred with 50.0 mL aliquots of a 0.01 mol L^{-1} NaCl solution using a simple batch method on an axial homogenizer. The initial pH of these aliquots ranged from 2.0 to 12.0. The pH was adjusted by the addition of dilute solutions of HCl and NaOH. The mixtures containing the material were stirred for 24 h. At the end of the agitation period, the final pH of the solutions was measured. A calibrated pH meter, PHS-3B (PHTEK, Brazil), was used to record the initial and final pH of the solutions.

2.5. Batch Adsorption Experiments

To gain insight into the adsorption capabilities of persimmon leaf powder and assess its suitability as a biosorbent, we explored critical parameters kinetic equilibrium, pH impact, and maximum adsorption capacity. Batch experiments were conducted by stirring 10 mg of the adsorbent powder with 1.80 mL of the metal solution within 2.0 mL Eppendorf tubes using an axial homogenizer. The material was subsequently filtered under pressure (to minimize contact between the metal species and the paper filter), and the supernatant was collected for metal content analysis. The analysis of the metal concentration in the collected solutions was performed by flame atomic absorption spectrometry (FAAS), after appropriate dilutions of the supernatants (using diluted HNO_3 solution). In each experiment, parameters such as contact time, pH, and analyte concentration were individually adjusted. Kinetic tests were performed to determine the minimum duration necessary for the material to attain equilibrium in adsorption kinetics. These experiments entailed the

mechanical agitation of the material with the analyte solution, spanning a time range of 1 to 240 min, conducted at room temperature. The concentrations of Cu(II) and Cd(II) in the solutions were set at 50 mg L^{-1} and 25 mg L^{-1}, respectively, while maintaining a pH of approximately 5.5. The specific influence of solution pH on the adsorption of copper and cadmium was evaluated. Adsorption experiments were conducted under different pH values to determine the optimal pH at which the material exhibited the highest adsorption capacity. These experiments involved mechanical agitation of Cu(II) and Cd(II) solutions at concentrations of 50 mg L^{-1} and 20 mg L^{-1}, respectively. The pH values of the Cu(II) and Cd(II) solutions were adjusted from 1 to 6, and the material was allowed to interact with the solutions for 120 min.

To determine the influence of the analyte concentration on the maximum adsorption capacity of the material, it was mechanically agitated with Cu(II) and Cd(II) solutions of different concentrations (1 to 400 mg L^{-1}). For these experiments, the pH of the Cu(II) and Cd(II) solutions was adjusted to approximately 5.5, and the stirring time of the material with these solutions was 120 min. All batch experiments were performed at a room temperature of approximately 25 °C. After determining the residual concentration of the metals in the diluted supernatants, the adsorption capacity for all experiments was calculated using Equation (1):

$$N_f = \frac{n_i - n_s}{m} \quad (1)$$

where n_i is the initial number of millimoles of the metal ion in the solution, n_s is the number of millimoles of the metal ion in the supernatant after extraction, and m is the mass of the adsorbent used (in grams).

3. Results and Discussion

3.1. Characterization of the Material

The morphology of the particles, their surface properties, and the chemical composition of the adsorbent were investigated using techniques such as scanning electron microscopy (SEM), energy-dispersive X-ray spectroscopy (EDX), elemental analysis of C, H, and N, ^{13}C nuclear magnetic resonance (^{13}C-NMR), infrared spectroscopy (FTIR), and point of zero charge (pH_{PZC}). In Figures 1 and 2, we can observe the spectra collected using the FTIR and ^{13}C-NMR techniques. In Figure 1, the infrared spectrum presents important bands related to the organic groups of the material, where it is possible to identify potential functional groups involved in the coordination of metal ions. The bands observed at 3405 and 2915 cm^{-1} are attributed to the stretching vibration of the O-H and C-H bonds, respectively. Anticipated bands are likely to appear because these clusters constitute the primary elements within cellulose, a significant component found in leaves.

The strong and broad O-H band is the result of this polymeric constituent. The C-H stretching band is derived from the primary and secondary carbons (CH_3 and CH_2). The prominent band at 1630 cm^{-1} can be attributed to the twisting vibration of the primary N-H bonds present in the amino acid structures. The infrared absorption bands observed at 1370 and 1320 cm^{-1} correlate with the stretching of the C-N bonds of aromatic amines found in the material. The absorption band located at 1030 cm^{-1} can be attributed to the symmetric stretching vibrations of the C-O bonds in the alcoholic groups. In the infrared spectrum, we cannot confirm the presence of carboxyl groups because the C=O stretching band generally observed in the wavelength range between 1760 and 1690 cm^{-1} is not present.

Figure 2 shows the ^{13}C-NMR spectrum of the pulverized material. The highest resonance, observed at 74.2 ppm, corresponds to the C-OH groups of flavonoid glycosides, which are the main non-structural constituents of persimmon leaves. This large resonance signal can also be assigned to the carbons of the C-O bonds present in the flavonoid and coumarin rings. The signal observed at 171.7 ppm can be attributed to COOH groups of fatty acids and terpenoids present in considerable amounts in the leaves [50]. A high resonance peak, observed at 168.0 ppm, may be associated with the carbons of the guanidine and carbamoyl groups present in the amino acids arginine and citrulline, respectively [51].

The observed resonances between 154.2 and 144.2 ppm may be related to the N=C-S groups found in thiamin [44].

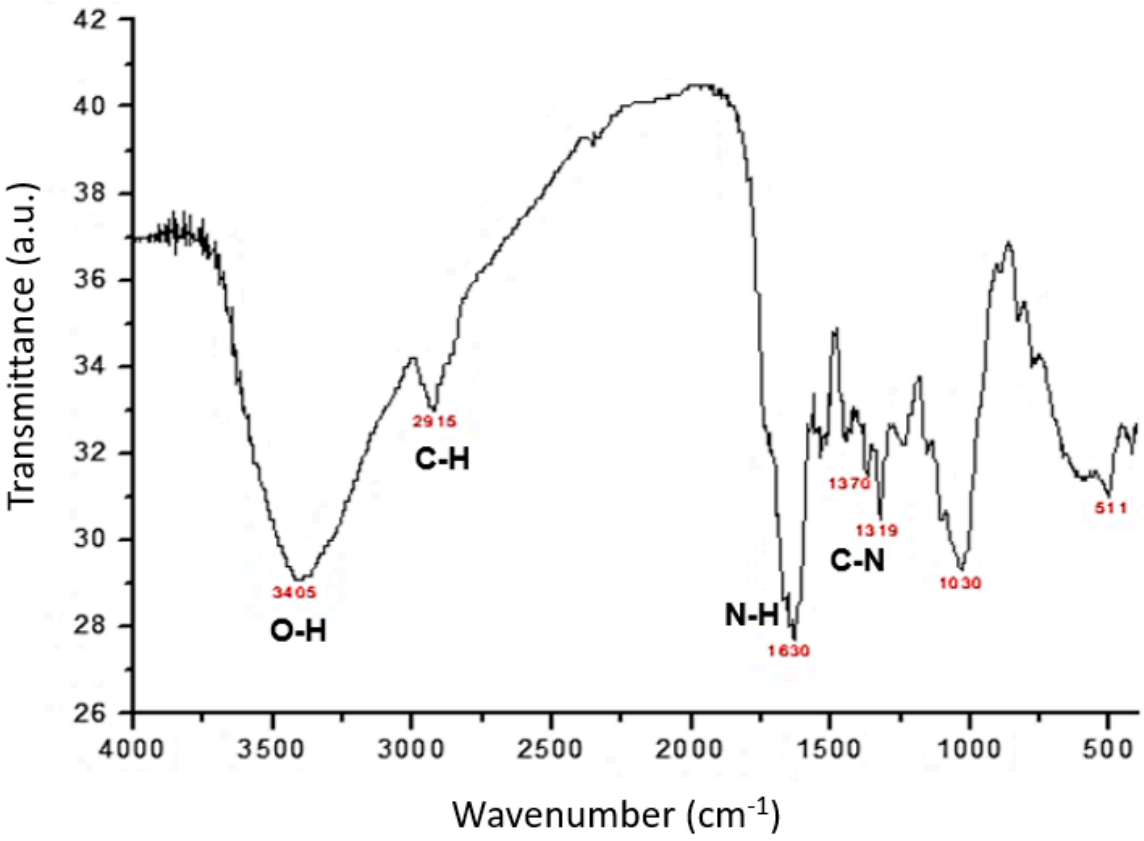


Figure 1. Infrared spectra of leaves of *Diospyros kaki* L.f.

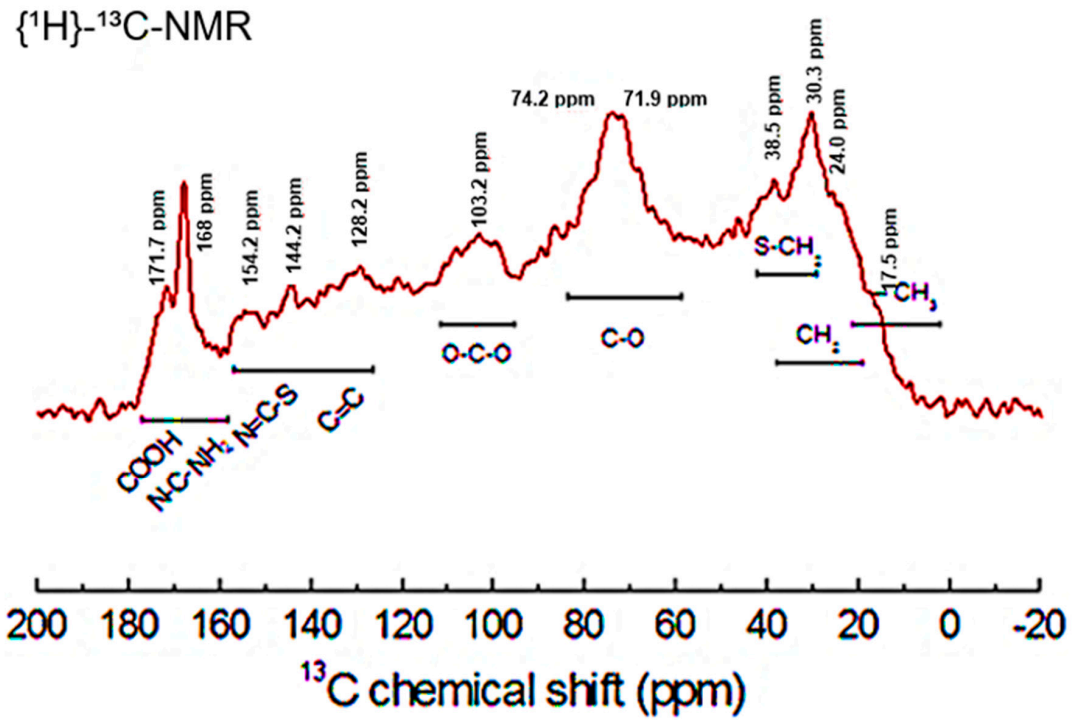


Figure 2. ^{13}C-NMR spectra of leaves of *Diospyros kaki* L.f.

The signal observed at 129.2 ppm is attributed to the presence of unsaturated aliphatic compounds (alkenes). This signal is also correlated with the unsaturated carbons (C=C) in aromatic compounds [52]. There is little evidence of the presence of nitrile (C≡N) bonds because of the low characteristic signal observed around 120 ppm. The resonance signal observed at 103.2 ppm corresponds to the anomeric carbons (O-C-O) of aldoses and ketoses [52]. The signal shown at 38.5 ppm is consistent with the S-CH_2 groups present in the amino acid methionine and cysteine [35]. A strong resonance can be observed at 30.3 ppm, which is attributed to the carbons (R_2CH_2) of saturated aliphatic compounds (alkanes), as well as the signal seen at 24.0 ppm. This large peak is expected in materials of vegetable origin, which contain a wide number of structural polysaccharides such as lignin and cellulose. We cannot verify the resonance of the carbons involved in the peptide bonds (C-N) because the characteristic signal around 60 ppm is not present.

Infrared (IR) analysis and nuclear magnetic resonance (NMR) are fundamental analytical techniques in the characterization of biosorbent materials, especially when studying the interaction of these materials with metallic species. Furthermore, concerning the groups that may be related to the adsorption process of metallic species, some of the key functional groups include carboxyl groups (COOH), amino groups (NH_2), hydroxyl groups (OH), and thiol groups (SH). These groups can form chemical bonds with metallic ions through ion exchange interactions, chemical coordination, or surface adsorption, and play a crucial role in the ability of a biosorbent material to effectively remove heavy metals or other metallic pollutants from aqueous solutions (Figure 3).

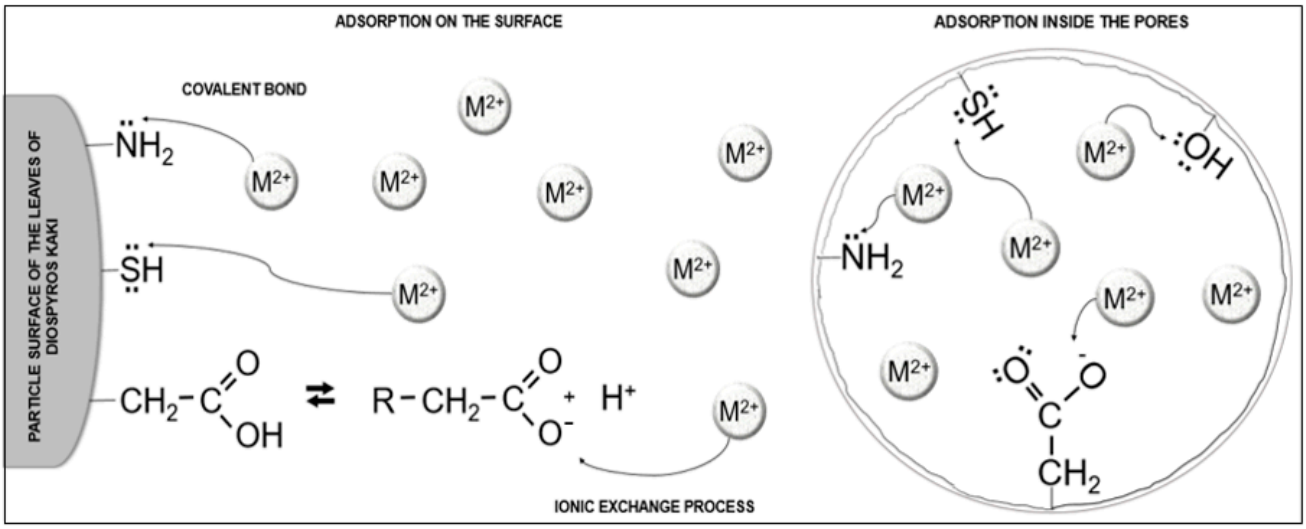


Figure 3. Schematic representation of possible interactions between the material surface functional groups and divalent metal cations. The arrow indicates the complexation of the metallic species.

The ground material was also analyzed by SEM to determine particle size homogeneity and particle morphology. According to Figure 4, the particle size is not homogeneous, and some particles have very irregular shapes. Furthermore, these particles exhibit a notably coarse microscopic texture characterized by irregular channels. This feature contributes to an increased surface area of the material and offers numerous adsorption sites for metal species.

The pore size distribution curve (Figure 5), displays a wide and non-uniform distribution of pores, featuring a mesoporous structure in the range of 350 Å to 400 Å, with a specific surface area of approximately 0.44 ± 0.015 m^2 g^{-1}.

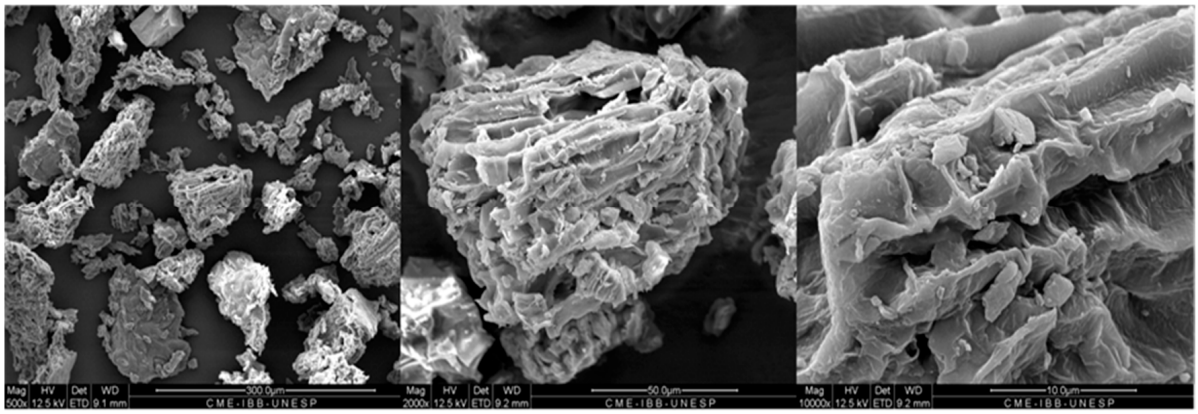


Figure 4. SEM images of the particles of the material. On the left (**a**) is an overview of the particles. In the middle, (**b**) we can see its irregular texture, and to the right (**c**) we have a detailed image of the pores and channels of the particle wall.

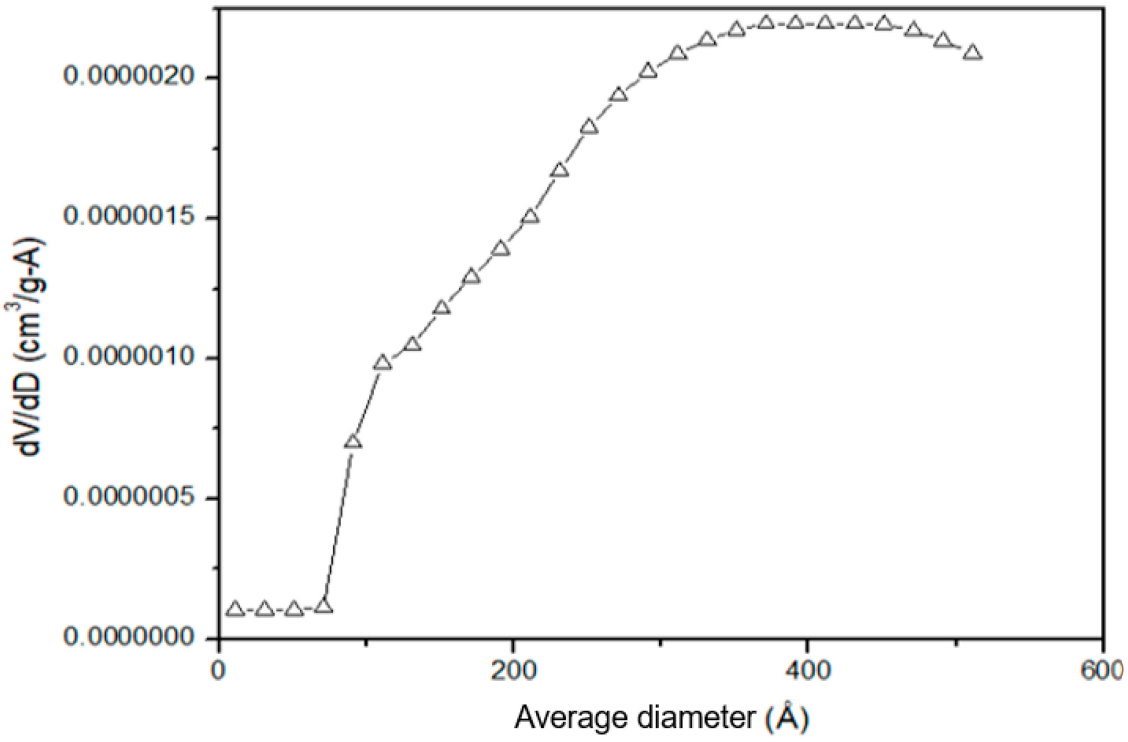


Figure 5. Pore size distribution obtained using the BET method.

EDX analysis was performed to map the distribution of the elements of interest onto the surface of the particles, and the collected elemental maps enabled the construction of Figure 6. The EDX maps indicate that N, O, S, and P are homogeneously distributed on the surface of the particles, and these elements are the main constituents of the groups of interest for the complexation of metal cations.

Elemental analysis showed that the leaves contain 44.87% C, 4.87% H, and 2.59% N (by weight). The presence of O and S atoms in the material was also the result of ^{13}C-NMR, which suggested the presence of molecules containing sulfur and oxygen.

An experiment was conducted to determine the point of zero charge (PZC) and the corresponding pH value at which the material has a net charge of zero (neutrality) on its surface (pH_{PZC}) as a function of the pH of the medium. Below pH_{PZC}, the material surface

becomes protonated, resulting in a positive charge (protonation of hydroxyl, carboxylic, and amine groups). On the contrary, when the medium's pH surpasses the material's pH_{PZC}, certain organic groups on the material's surface release their hydrogen ions, resulting in a negative charge. As a result, in the presence of metal cations at acidic pH levels, electrostatic repulsion occurs between the cations and the positively charged surface of the adsorbent, leading to diminished adsorption of these metal species. Conversely, at elevated pH values, the adsorption of cations may be promoted because of the material negatively charged surface. Nonetheless, contingent on the concentration of hydroxide ions in the medium, they can engage in solvation with metal cations, impeding their complexation by the organic groups present on the material surface. Then, we can conclude that the optimal pH for the adsorption of the metal cations is the pH at which the overall surface charge of the adsorbent is neutral, which is referred to as the point of zero charge (PZC). The data obtained from the PZC experiment were used to construct Figure 7, and pH_{PZC} is determined by the point where the experimental curve (initial pH versus final pH) intersects the line represented by x = y (initial pH = final pH). From the graph, we can observe that the pH_{PZC} for the persimmon leaf powder is 5.1. As discussed earlier, when the pH of the medium is below 5.1, the particles' surface will be positively charged, whereas at higher pH values, the surface of the adsorbent will exhibit a negative charge. Because the pH_{PZC} is slightly acidic, it indicates a prevalence of acidic groups on the material surface [21].

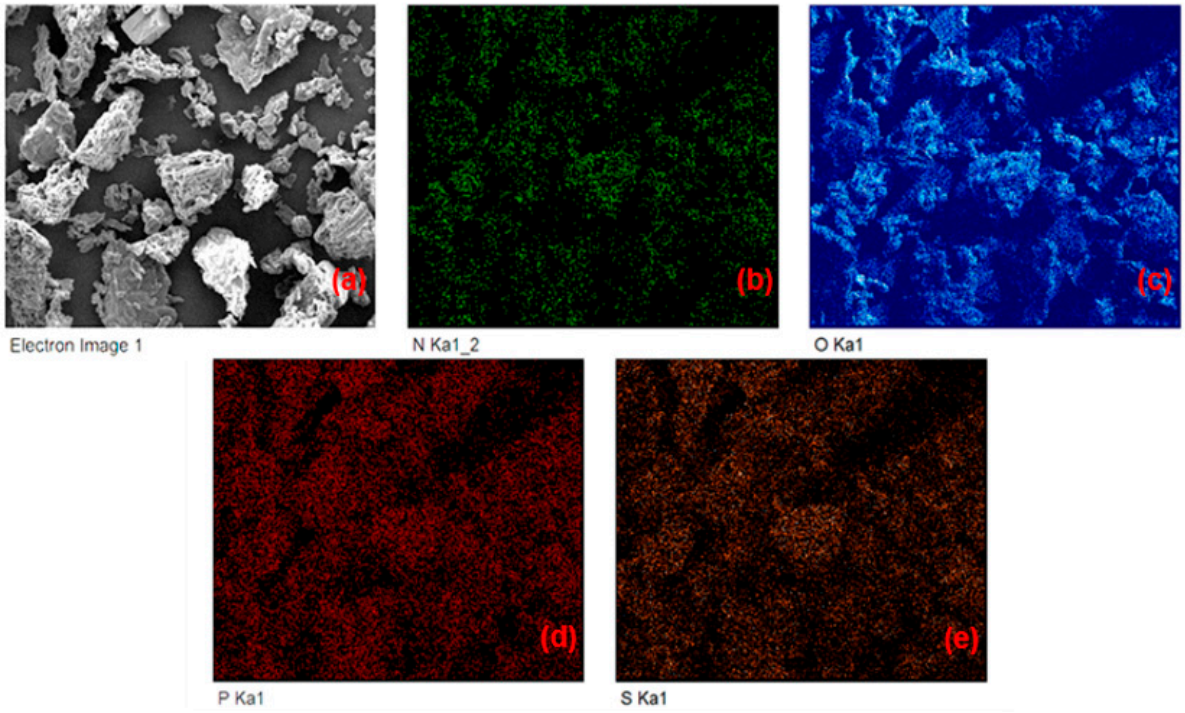


Figure 6. EDX analysis of persimmon leaves (compositional maps) for nitrogen (**b**), oxygen (**c**), phosphorus (**d**), and sulfur (**e**) elements. The electronic image of the region used to obtain the EDX analysis is also presented in (**a**).

3.2. Batch Adsorption Experiments

3.2.1. Adsorption Kinetics

Through kinetic experiments, we were able to establish the minimum duration of dynamic contact necessary for the material to achieve equilibrium with the metal solution. As shown in Figure 8 (inset), the material exhibits rapid kinetics, and the adsorption equilibrium is reached within 5 min for both metals. This indicates that the structure of the leaves provides high accessibility for the metal cations to coordinate with their adsorption sites. It is important to note that the rapid kinetics of an adsorbent is highly desirable, making the material very attractive for analytical and decontamination purposes.

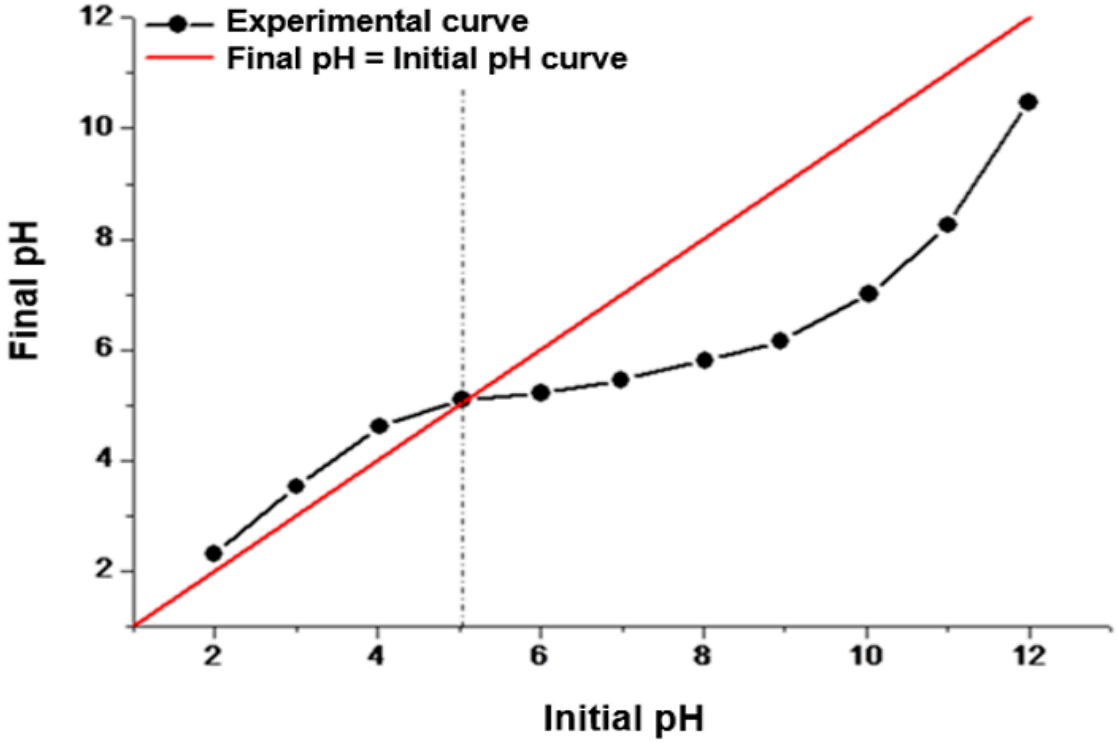


Figure 7. Determination of the point of zero charge (pH_{PZC}) of the surface of particles of the persimmon leaves.

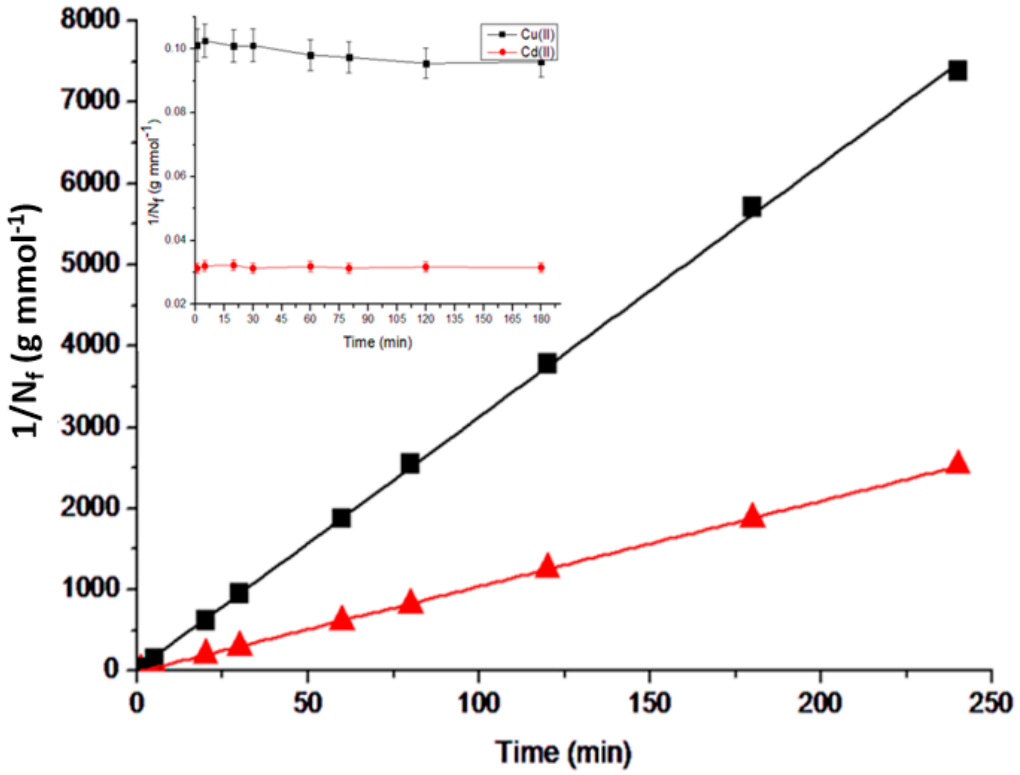


Figure 8. Linearization of the kinetic data according to the pseudo-second-order kinetic model, and the adsorption isotherms obtained for Cu(II) and Cd(II) (inset graph) at room temperature (25 °C). Initial concentrations of Cu(II) and Cd(II) solutions: 50 and 25 mg L^{-1}, respectively; mass of adsorbent used: 10.0 mg; solution pH ~ 5.5.

According to the literature, it is incorrect to use simple kinetic equations such as first- and second-order models to describe the adsorption process on heterogeneous surfaces [53]. Therefore, the experimental kinetic data obtained for Cu(II) and Cd(II) were applied to the linear kinetic model of pseudo-second order. This model suggests that the metal extraction process occurs through the covalent coordination of non-bonding electron pairs of atoms present on the surface of the adsorbent. The linearized form of the pseudo-second-order kinetic model is represented by Equation (2):

$$\frac{t}{N_{ft}} = \frac{1}{KN_e^2} + \frac{1}{N_e}t \quad (2)$$

where N_{ft} represents the adsorption capacity as a function of time (mmol g^{-1}); N_e corresponds to the adsorption capacity at equilibrium (mmol g^{-1}); K is the kinetic constant of the pseudo-second order (g $mmol^{-1}$ min^{-1}), and t is the contact time in each experiment (minutes). By plotting t/N_{ft} versus t, linearized kinetic isotherms were generated for the studied metal species, as depicted in Figure 8. We can observe a great agreement between the experimental data and the pseudo-second-order kinetic model, as evidenced by the high coefficients of linear correlation obtained (r^2 = 0.9999 for Cu(II) and r^2 = 0.9996 for Cd(II)). Considering an equation of the form $y = Bx + A$, the linear equations obtained for Cu(II) and Cd(II) are $y = 10.539x - 11.566$ and $y = 31.062x + 22.330$, respectively, where $y = t/N_{ft}$ and $x = t$. According to Equation (2), $B = 1/N_e$ and $A = 1/(K\,N_e{}^2)$, by substituting the respective angular and linear coefficients for both metals, it was possible to calculate N_e and K for each species, resulting in N_e = 0.0948 mmol g^{-1} and $K = -9.6031$ g $mmol^{-1}$ min^{-1} for Cu(II), and N_e = 0.0321 mmol g^{-1} and K = 43.208 g $mmol^{-1}$ min^{-1} for Cd(II). Another piece of evidence that confirms the good agreement with this model is the similarity between the experimental adsorption capacity values (observed when the kinetic isotherms reach the highest adsorption capacity) and the calculated values (obtained from the mathematical model).

3.2.2. Effect of pH of the Medium

The influence of pH on the adsorption process of Cu(II) and Cd(II) ions was investigated in solutions with pH values ranging from 1 to 6, as the concentration of H^+ species can affect the reaction equilibrium due to the protonation of the adsorption sites. Solutions with pH values higher than six were not tested because of the risk of hydrolysis reactions involving metal cations, which could compromise the adsorption process. The data obtained are plotted in Figure 9.

Both metal species exhibit the lowest adsorption capacities at pH values of two or lower. However, as the pH of the medium increases, adsorption becomes more effective. The highest metal adsorption was observed at pH values of 4.0 for Cu(II) and 3.0 for Cd(II). Such behavior is commonly observed in metal adsorption processes. At low pH values, the concentration of hydronium ions (H_3O^+) is sufficiently high for the H^+ species to compete with the metal ions for the adsorption sites. This effect intensifies at the lowest pH values. The size of the H^+ ions also plays a significant role in this competition, as their smaller size provides greater mobility in the medium. This property gives the H^+ ions an advantage in reaching the adsorption sites compared to larger metal ions such as Cu^{2+} and Cd^{2+} [21]. Consequently, the surface of the material becomes positively charged, leading to the repulsion of the metal ions present in the medium. As a result, metal adsorption was significantly compromised in low-pH media. As the pH increases and approaches neutrality, this effect becomes less intense as the concentration of hydronium ions decreases, allowing for the adsorption of metal ions. Because the material is capable of adsorbing metal ions over a wide pH range, it would be suitable for application in the solid-phase extraction of Cu(II) and Cd(II) from effluents, as well as for the decontamination of drinking water.

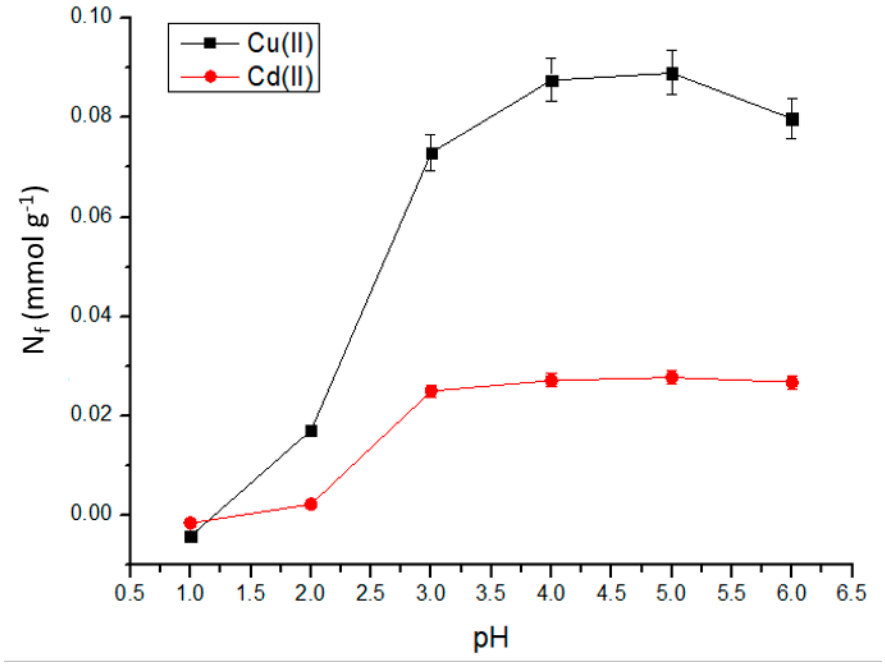


Figure 9. Effect of pH on adsorption of Cu(II) and Cd(II) in aqueous medium at room temperature (25 °C). Initial concentrations of Cu(II) and Cd(II) solutions: 50 and 20 mg L^{-1}, respectively; stirring time: 120 min; mass of adsorbent used: 10.0 mg.

3.2.3. Maximum Adsorption Capacity

Under optimal pH and contact time conditions, an experiment was conducted to determine the maximum adsorption capacity of the material as a function of Cu(II) and Cd(II) concentrations. The adsorption isotherms were plotted using the analyte concentrations and their respective N_f values (Figure 10).

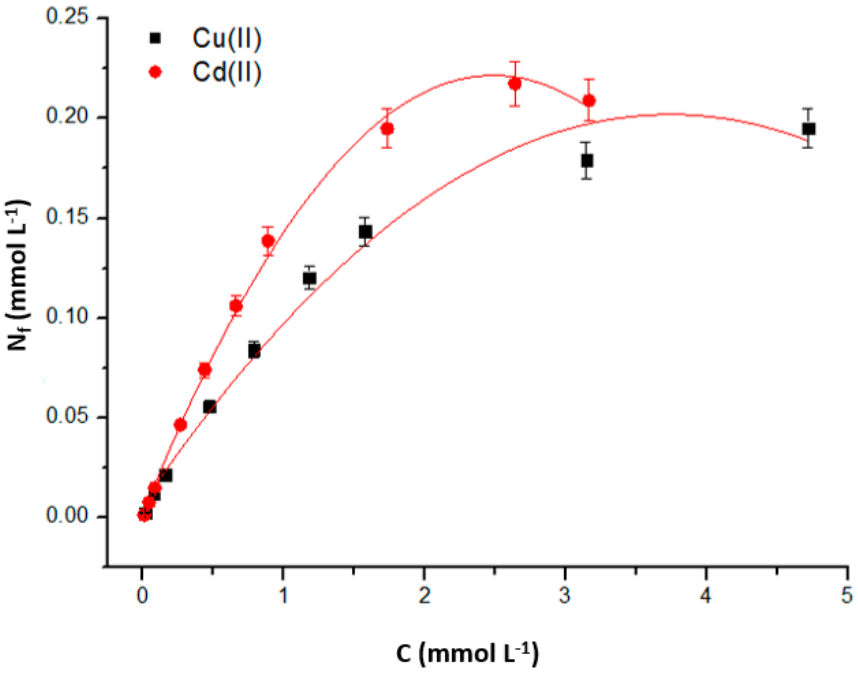


Figure 10. Adsorption isotherms of Cu(II) and Cd(II) at room temperature (25 °C). Stirring time: 120 min; mass of adsorbent used: 10.0 mg; solution pH ~ 5.5.

As observed, the graphical representation of the data shows maximum adsorption capacity (N_{fmax}) values of approximately 0.19 mmol L^{-1} for Cu(II) and 0.21 mmol L^{-1} for Cd(II). To further understand the adsorption process occurring on the material, the experimental data of the isotherms were fitted to the linearized Langmuir and Freundlich models. The Langmuir model quantitatively describes the formation of an adsorbate monolayer on the surface of an adsorbent, representing the equilibrium of adsorbate distribution between the solid and liquid phases. The Langmuir isotherm is widely used in biosorption assays of pollutants from aqueous solutions [54]. The linear form of the Langmuir isotherm is given by Equation (3) [55,56].

$$\frac{C_s}{N_f} = \frac{C_s}{N_s} + \frac{1}{N_s b} \tag{3}$$

In this expression, C_s represents the equilibrium concentration of the supernatant (mmol L^{-1}); N_f is the amount of metal ions adsorbed on the material surface (mmol g^{-1}); N_s is the maximum amount of metal ions adsorbed per gram of adsorbent (mmol g^{-1}), which is related to the number of available adsorption sites, and b (L $mmol^{-1}$) is a constant that reflects the affinity of the metal ions with the solid matrix and the adsorption energy. In contrast, the Freundlich model is applicable to adsorption on heterogeneous surfaces and considers that adsorption occurs in multilayers with interactions between the adsorbed molecules [54]. The linearized form of the Freundlich isotherm is given by Equation (4) [57]:

$$\log q_e = \log k_f + \frac{1}{n} \log C_e \tag{4}$$

where C_e represents the equilibrium concentration of the metal species (mmol L^{-1}); q_e is the number of metal ions adsorbed per gram of adsorbent at equilibrium (mmol g^{-1}); k_f ($mmol^{1-(1/n)}$ $L^{1/n}$ g^{-1}) is the Freundlich constant that relates to the adsorption capacity, and n is a dimensionless constant that describes the intensity of the adsorption process. The values of b and N_s can be determined from the slopes and intercepts of the linear plots of C_s/N_f versus C_s (Langmuir isotherm), whereas the values of k_f and n are calculated from the intercepts and slopes of the plot of $\log q_e$ versus $\log C_e$. The values of the constants (b, k_f, and n), and the correlation coefficients (r^2) generated by the linearization of the experimental data are listed in Table 1.

Table 1. Isotherm parameters for the adsorption of Cu(II) and Cd(II).

Metal	N_{fmax} (exp.) (mmol g^{-1})	Langmuir			Freundlich		
		b (L $mmol^{-1}$)	N_s (calc.) (mmol g^{-1})	r^2	K_f ($mmol^{1-(1/n)}$ $L^{1/n}$ g^{-1})	n	r^2
Cu(II)	0.19	2.84	0.21	0.95	0.89	1.82	0.93
Cd(II)	0.23	32.5	0.22	0.99	4.90	2.58	0.90

Based on the obtained linear correlation values (r^2), the Langmuir linearized model has proven to be the most suitable for fitting the experimental data of both metal species. This model exhibited excellent agreement with the adsorption data, as indicated by the high coefficients of linear correlation. Using the best-fit straight-line equations, it was possible to calculate the maximum adsorption capacity of the material (N_s) for Cu(II) and Cd(II) based on their angular coefficients ($B = 1/N_s$). Considering the similarity between these N_s values and the N_{fmax} values determined in the adsorption isotherms, we can infer that a significant portion of the available adsorption sites on the material surface area is involved in the coordination of the metal species. The maximum adsorption capacity of the persimmon leaves is very similar for Cu(II) and Cd(II). The high efficiency of metal removal can be explained by the significant presence of sulfur and nitrogen in the material in question. These elements play important roles as soft and intermediate

Lewis bases, respectively, which means that they can donate electron pairs to interact with metal ions in solution. This phenomenon has been consistently observed in previous studies, as mentioned by [58]. The presence of these bases suggests that the material has great potential for use in the solid-phase extraction of a wide variety of metal species, making it a promising choice for applications in the purification and recovery of metals from aqueous solutions. Concentrations above 400 mg L^{-1} were not evaluated because of the difficulty in preparing more concentrated solutions of copper and cadmium at pH levels above six. Increased concentrations of these metal species result in hydrolysis reactions and precipitate formation.

To compare the performance of persimmon leaf powder with that of other adsorbents in terms of Cu(II) and Cd(II) adsorption, Table 2 was constructed. Despite having a similar adsorption capacity, persimmon leaves require a simple treatment before their application in solid-phase extraction. This results in low-cost procedures and aligns with the principles of green chemistry, as the production of this adsorbent does not generate any toxic waste. Furthermore, it is derived from a renewable source and can be used for environmental purposes.

Table 2. Comparison of the maximum adsorption capacity of persimmon leaves with other biosorbents (maximum adsorption values in milligrams of metal per gram of dry adsorbent).

Material	N_s (mg g^{-1})		Bibliography
	Cu(II)	Cd(II)	
Pata-de-vaca leaves	-	8.45	[21]
Cassava root husks	8.90	-	[35]
Corn leaf	5.66	7.98	[44]
Cassava root husks	-	12.25	[20]
Onosma bracteatum	-	21.66	[59]
P. volubilis shell	9.70	-	[60]
Pine cone shell	6.81	-	[61]
D. bipinnata leaves	-	15.22	[62]
B. aundinacea leaves	-	19.70	[62]
Coffee grounds	-	15.65	[63]
Wheat straw	11.44	14.61	[64]
Eucalyptus bark	-	14.53	[65]
Sunflower waste	-	23.60	[66]
D. carota residues	8.88	-	[67]
Maple wood	9.51	-	[68]
Areca catechu heartwood	-	10.66	[69]
Glebionis coronaria	-	18.31	[70]
Cashew nut shell	-	11.23	[71]
Marula seed husk	10.20	-	[72]
Sugarcane bagasse	9.48	-	[73]
Watermelon rind	5.73	-	[73]
Lentil shells	9.59	-	[74]
Gooseberry fruit	9.52	-	[75]
Orange peel	-	15.27	[76]
Groundnut husk	9.26	-	[77]
Rice straw	-	13.90	[78]
Olive stone	-	11.72	[79]
Sorghum stalk	13.32	-	[80]
Bamboo charcoal	-	12.08	[81]
Persimmon leaves	13.54	24.17	This study

The table showcases several materials that share similarities with persimmon leaves, the subject of the referenced study, with its data appearing in the final row. Persimmon leaves are noteworthy because of their abundant and easily obtainable nature. Unlike less available or more challenging-to-acquire materials, such as specific synthetic chemicals or other materials of rare origin, persimmon leaves are readily accessible in many

regions. Moreover, the ease of procuring persimmon leaves renders them an attractive choice for applications involving the adsorption of metals in aqueous solutions. This is especially significant when considering the necessity for scalability in practical scenarios. The abundant supply of persimmon leaves can render this solution both economically and environmentally friendly, allowing for its extensive implementation in the removal of metals from liquid effluents or contaminated solutions. Therefore, the selection of persimmon leaves as an adsorbent in this study not only yields noteworthy outcomes in the context of copper and cadmium adsorption but also underscores a crucial facet of environmental research and metal removal technology. This facet revolves around harnessing naturally abundant and readily accessible resources to tackle intricate environmental challenges. This approach can be regarded as sustainable and economically viable, thereby contributing to the advancement of research and the development of more effective and accessible water and effluent treatment technologies.

4. Conclusions

Persimmon leaves represent a low-cost alternative adsorbent for the removal of toxic metals from aqueous media. This material is abundant and can be easily processed into a fine powder using simple procedures. Grinding and pulverizing the leaves result in a porous material that does not require prior functionalization steps for the uptake of metal ions. It can be directly applied to remediate metal species in aqueous solutions. Characterization of the powdered leaves revealed the presence of functional groups that act as Lewis bases and play a crucial role in the chemisorption of Cu(II) and Cd(II) ions. The material exhibited rapid kinetics and proved to be effective over a wide pH range (3–6). Its adsorption behavior was best described by the Langmuir adsorption model, and its maximum adsorption capacity was comparable to that of many other biosorbents.

Future prospects for persimmon leaves in the field of metal removal from aqueous media include further exploration of their potential in real-world applications. It is important to conduct long-term studies to assess their durability and performance under varying environmental conditions. In addition, research could focus on optimizing the processing methods to further enhance their adsorption capacity and efficiency. Investigating the regenerability of persimmon leaf-based adsorbents and exploring their use in large-scale water treatment processes would be valuable areas of future research. Furthermore, the combination of persimmon leaves with other materials or modification techniques may offer opportunities to improve their selectivity for specific metal ions. Overall, persimmon leaves hold promise as a cost-effective and environmentally friendly solution for the removal of toxic metals from aqueous environments, and their continued exploration in various applications is justified.

Author Contributions: Conceptualization, R.M.G., A.C.P.d.S., A.d.O.J. and M.H.P.W.; methodology, R.M.G. and A.C.P.d.S.; software, J.F.S. and M.A.U.M.; validation, R.M.G., J.F.S. and M.A.U.M.; formal analysis, M.J.S. and V.d.A.P.; investigation, R.M.G.; resources, M.J.S., J.F.S., V.d.A.P., M.A.U.M. and G.R.C.; data curation, R.M.G., A.C.P.d.S., A.d.O.J., M.H.P.W., M.J.S., J.F.S., V.d.A.P., M.A.U.M. and G.R.C.; writing—original draft preparation, G.R.C., A.C.P.d.S. and A.d.O.J.; writing—review and editing, G.R.C. and A.C.P.d.S.; visualization, M.J.S. and V.d.A.P.; supervision, G.R.C.; project administration, G.R.C.; funding acquisition, G.R.C. All authors have read and agreed to the published version of the manuscript.

Funding: The APC was funded by CNPq (Proc. 312361/2021-1) and PROPG/UNESP (Edital: 69/2023).

Data Availability Statement: Data are contained within the article.

Conflicts of Interest: The authors declare no conflicts of interest.

References

1. Carneiro, P.A.; Umbuzeiro, G.A.; Oliveira, D.P.; Zanoni, M.V.B. Assessment of water contamination caused by a mutagenic textile effluent/dyehouse bearing disperse dyes. *J. Hazard. Mater.* **2010**, *174*, 689–699. [CrossRef] [PubMed]
2. Minello, M.C.S.; Paço, A.L.; Martines, M.A.U.; Caetano, L.; Santos, A.; Padilha, P.M.; Castro, G.R. Sediment grain size distribution and heavy metals determination in a dam on the Parana River at Ilha Solteira, Brazil. *J. Environ. Sci. Health* **2009**, *44*, 861–865. [CrossRef] [PubMed]
3. García-Sánchez, A.; Pérez-Esteban, J.; Escolástico, C.; Martínez-Álvarez, R.M.; Ibáñez, R.; Muñoz, M.; VILLAFRANCA-SÁNCHEZ, M. Assessment of selenium (IV) and (VI) levels in potable, irrigation, and wastewater samples from an industrial area in southeastern Spain. *Environ. Sci. Pollut. Res.* **2022**, *29*, 4419–4428.
4. Gupta, N.; Khan, D.K. Distribution, health risk assessment and statistical source identification of heavy metals in surface water of River Ganges Basin, India. *Sci. Total Environ.* **2020**, *706*, 135873.
5. Zhang, Z.; Wang, Q.; Yao, L. A review on ecological risk assessment and potential health risk of toxic heavy metals in abandoned mining areas. *Environ. Sci. Pollut. Res.* **2021**, *28*, 10843–10856.
6. Almeida, E.; Soares, A.M.; Figueira, E. Bioaccumulation of cadmium, selenium, and zinc in native oysters (*Crassostrea angulata*) from a contaminated estuary: Implications for environmental monitoring and human health. *Environ. Sci. Pollut. Res.* **2018**, *25*, 21311–21320.
7. Reeve, R.N. *Introduction to Environmental Analysis*; John Wiley & Sons Ltd.: Chichester, UK, 2002.
8. Baird, C.; Cann, M. *Química Ambiental*, 4th ed.; Bookman: Porto Alegre, Brazil, 2011.
9. Manahan, S.E. *Environmental Science Technology and Chemistry*; CRC Press LLC: Boca Raton, FL, USA, 2000.
10. Cao, W.; Zhang, M.; Ma, W.; Huang, C. Multifunctional electrospun nanofibrous membrane: An effective method for water purification. *Sep. Purif. Technol.* **2023**, *327*, 124952. [CrossRef]
11. Posa, M.; Bhattarai, A.; Khan, J.M.; Saha, B.; Kumar, D. Impact of double headed geminis on leucine and nihydrin reaction in buffer solvent. *Colloids Surf. A Physicochem. Eng. Asp.* **2023**, *674*, 131951. [CrossRef]
12. Sun, H.; Dai, Q.; Liu, J.; Zhou, T.; Chen, M.; Cai, Z.; Zhu, X.; Fu, B. $BiVO_4$–Deposited MIL–101–NH2 for Efficient Photocatalytic Elimination of Cr(VI). *Molecules* **2023**, *28*, 1218. [CrossRef]
13. Alcântara, I.L.; Roldan, P.S.; Castro, G.R.; Moraes, F.V.; Silva, F.A.; Padilha, C.F.; Oliveira, J.D.; Padilha, P.M. Determination of cadmium in river water samples by flame AAS after on-line preconcentration in mini-column packed with 2-aminothiazole-modified silica gel. *Anal. Sci.* **2004**, *20*, 1029–1032. [CrossRef]
14. Madrakian, T.; Zolfigol, M.A.; Solgi, M. Solid-phase extraction method for preconcentration of trace amounts of some metal ions in environmental samples using silica gel modified by 2,4,6-trimorpholino-1,3,5-triazin. *J. Hazard. Mater.* **2008**, *160*, 468–472. [CrossRef] [PubMed]
15. Mahmoud, M.E.; Hafez, O.F.; Alrefaay, A.; Osman, M.M. Performance evaluation of hybrid inorganic/organic adsorbents in removal and preconcentration of heavy metals from drinking and industrial wastewater. *Desalination* **2010**, *253*, 9–15. [CrossRef]
16. Ferreira, G.; Caetano, L.; Castro, R.S.D.; Padilha, P.M.; Castro, G.R. Synthesis, characterization, and application of modified silica in the removal and preconcentration of lead ions from natural river water. *Clean Technol. Environ.* **2011**, *13*, 397–402. [CrossRef]
17. Prado, A.G.S.; Pescara, I.C.; Evangelista, S.M.; Holanda, M.S.; Andrade, R.D.; Suarez, P.A.Z.; Zara, L.F. Adsorption and preconcentration of divalent metal ions in fossil fuels and biofuels: Gasoline, diesel, biodiesel, diesel-like and ethanol by using chitosan microspheres and thermodynamic approach. *Talanta* **2011**, *84*, 759–765. [CrossRef] [PubMed]
18. Filho, E.C.S.; Lima, L.C.B.; Silva, F.C.; Souza, K.S.; Fonseca, M.G.; Santana, S.A.A. Immobilization of ethylene sulfide in aminated cellulose for removal of the divalent cations. *Carbohydr. Polym.* **2013**, *92*, 1203–1210. [CrossRef]
19. Hajiaghababaei, L.; Tajmiri, T.; Badiei, A.; Ganjali, M.R.; Khaniani, E.; Ziarani, G.M. Heavy metals determination in water and food samples after preconcentration by a new nanoporous adsorbent. *Food Chem.* **2013**, *141*, 1916–1922. [CrossRef]
20. Jorgetto, A.O.; Silva, A.C.P.; Cavecci, B.; Barbosa, R.C.; Utrera, M.A.; Castro, G.R. Cassava Root Husks as a Sorbent Material for the Uptake and Pre-concentration of Cadmium(II) from Aqueous Media. *Orbital Electron. J. Chem.* **2013**, *5*, 206–212.
21. Jorgetto, A.O.; Silva, A.C.P.; Wondracek, M.H.P.; Silva, R.I.V.; Velini, E.D.; Saeki, M.J.; Pedrosa, V.A.; Castro, G.R. Multilayer adsorption of Cu(II) and Cd(II) over Brazilian Orchid Tree (Pata-de-vaca) and its adsorptive properties. *Appl. Surf. Sci.* **2015**, *345*, 81–89. [CrossRef]
22. Ahmad, M.A.; Ahmad, N. Effective removal of cadmium and zinc from wastewater using agricultural waste-based activated carbon: Adsorption isotherm, kinetics, and thermodynamic studies. *Environ. Sci. Pollut. Res.* **2022**, *29*, 5292–5306.
23. Gupta, V.K.; Ali, I.; Saleh, T.A.; Nayak, A.; Agarwal, S. Chemical treatment technologies for waste-water recycling—An overview. *RSC Adv.* **2012**, *2*, 6380–6388. [CrossRef]
24. Mellah, A.; Chegrouche, S.; Barkat, M. The removal of uranium (VI) from aqueous solutions onto activated carbon: Kinetic and thermodynamic investigations. *J. Colloid Interface Sci.* **2006**, *296*, 434–441. [CrossRef] [PubMed]
25. Peng, X.W.; Zhong, L.X.; Ren, J.L.; Sun, R.C. Highly effective adsorption of heavy metal ions from aqueous solutions by macroporous Xylan-rich hemicelluloses based hydrogel. *J. Agric. Food Chem.* **2012**, *60*, 3909–3916. [CrossRef] [PubMed]
26. Liu, C.C.; Wang, M.K.; Li, Y.S. Removal of nickel from aqueous solution using wine processing waste sludge. *J. Ind. Eng. Chem.* **2005**, *44*, 1438–1445. [CrossRef]
27. Walcarius, A.; Mercier, L. Mesoporous organosilica adsorbents: Nanoengineered materials for removal of organic and inorganic pollutants. *J. Mater. Chem.* **2010**, *20*, 4478–4511. [CrossRef]

28. Naiya, T.K.; Bhattacharya, A.K.; Das, S.K. Adsorptive removal of Cd(II) ions from aqueous solutions by rice husk ash. *Environ. Prog. Sustain. Energy* **2009**, *28*, 535–546. [CrossRef]
29. Singha, B.; Das, S.K. Adsorptive removal of Cu(II) from aqueous solution and industrial effluent using natural/agricultural wastes. *Colloids Surf. B Biointerfaces* **2013**, *107*, 97–106. [CrossRef] [PubMed]
30. Souza, E.J.; Cristante, V.M.; Padilha, P.M.; Jorge, S.M.A.; Martines, M.A.U.; Silva, R.I.V.; Carmo, D.R.; Castro, G.R. Attachment of 2,2-bypiridine onto a silica gel for application as a sequestering agent for copper, cadmium and lead ions from an aqueous medium. *Pol. J. Chem. Technol.* **2011**, *13*, 28–33. [CrossRef]
31. Castro, R.S.D.; Caetano, L.; Ferreira, G.; Padilha, P.M.; Saeki, M.J.; Zara, L.F.; Martines, M.A.U.; Castro, G.R. Banana peel applied to the solid-phase extraction of copper and lead from river water: Preconcentration of metal ions with a fruit waste. *Ind. Eng. Chem. Res.* **2011**, *50*, 3446–3451. [CrossRef]
32. Martins, A.E.; Pereira, M.S.; Jorgetto, A.O.; Martines, M.A.U.; Silva, R.I.V.; Saeki, M.J.; Castro, G.R. The reactive surface of Castor leaf [*Ricinus communis* L.] powder as a green adsorbent for the removal of heavy metals from natural river water. *Appl. Surf. Sci.* **2013**, *276*, 24–30. [CrossRef]
33. Saad, E.M.; Elshaarawy, R.F.; Mahmoud, S.A.; El-Moselhy, K.M. New ulva lactuca algae based chitosan bio-composites for bioremediation of Cd(II) ions. *J. Bioresour. Bioprod.* **2021**, *6*, 223–242. [CrossRef]
34. Sepehri, S.; Kanani, E.; Abdoli, S.; Rajput, V.D.; Minkina, T.; Asgari LAJAYER, B. Pb(II) Removal from Aqueous Solutions by Adsorption on Stabilized Zero-Valent Iron Nanoparticles—A Green Approach. *Water* **2023**, *15*, 222. [CrossRef]
35. Jorgetto, A.O.; Silva, R.I.V.; Saeki, M.J.; Barbosa, R.C.; Martines, M.A.U.; Jorge, S.M.A.; Silva, A.C.P.; Schneider, J.F.; Castro, G.R. Cassava root husks powder as green adsorbent for the removal of Cu(II) from natural river water. *Appl. Surf. Sci.* **2014**, *288*, 356–362. [CrossRef]
36. Gurgel, L.V.A.; Gil, L.F. Adsorption of Cu(II), Cd(II) and Pb(II) from aqueous single metal solutions by succinylated twice-mercerized sugarcane bagasse functionalized with triethylenetetramine. *Water Res.* **2009**, *43*, 4479–4488. [CrossRef] [PubMed]
37. Gönen, F.; Serin, D.S. Adsorption study on orange peel: Removal of Ni(II) ions from aqueous solution. *Afr. J. Biotechnol.* **2012**, *11*, 1250–1258.
38. Zhang, Y.; Li, X.; Zhou, Y. Application of peanut shell biochar for heavy metal removal from wastewater: A review. *Environ. Sci. Pollut. Res.* **2021**, *28*, 4802–4817.
39. Gonzales, M.H.; Araújo, G.C.L.; Pelizaro, C.B.; Menezes, E.A.; Lemos, S.G.; Souza, G.B.; Nogueira, A.R.A. Coconut coir as biosorbent for Cr(VI) removal from laboratory wastewater. *J. Hazard. Mater.* **2008**, *159*, 252–256. [CrossRef]
40. Gundoğdu, A.; Özdes, D.; Duran, C.; Bulut, V.N.; Soylak, M.; Senturk, H.B. Biosorption of Pb(II) ions from aqueous solution by pine bark (*Pinus brutia* Ten.). *Chem. Eng. J.* **2009**, *153*, 62–69. [CrossRef]
41. Hossain, M.A.; Ngo, H.H.; Guo, W.S.; Setiadi, T. Adsorption and desorption of copper(II) ions onto garden grass. *Bioresour. Technol.* **2012**, *121*, 386–395. [CrossRef]
42. Naiya, T.K.; Bhattacharya, A.K.; Das, S.K. Removal of Cd(II) from aqueous solutions using clarified sludge. *J. Colloid Interface Sci.* **2008**, *325*, 48–56. [CrossRef]
43. Souza, F.W.; Oliveira, A.G.; Ribeiro, J.P.; Rosa, M.F.; Keukeleire, D.; Nascimento, R.F. Green coconut shells applied as adsorbent for removal of toxic metal ions using fixed-bed column technology. *J. Environ. Manag.* **2010**, *91*, 1634–1640. [CrossRef]
44. Silva, A.C.P.; Jorgetto, A.O.; Wondracek, M.H.P.; Saeki, M.J.; Schneider, J.F.; Pedrosa, V.A.; Martines, M.A.U.; Castro, G.R. Characterization of corn (*Zea mays*) leaf powder and its adsorption properties regarding Cu(II) and Cd(II) from aqueous samples. *BioResources* **2015**, *10*, 1099–1114. [CrossRef]
45. Kobya, M. Adsorption, kinetic and equilibrium studies of Cr(VI) by hazelnut shell activated carbon. *Adsorpt. Sci. Technol.* **2004**, *22*, 51–64. [CrossRef]
46. Matsumoto, J.; Sato, M. Seasonal Changes in Nutrient Composition of Persimmon (*Diospyros kaki* L. F.) *Leaves*. *J. Jpn. Soc. Hortic. Sci.* **1997**, *66*, 421–428.
47. Vaghetti, J.C.P. Utilização de Biossorventes Para Remediação de Efluentes Aquosos Contaminados Com Íons Metálicos. *Data de defesa:* 2009. 84 f. Ph.D. Thesis, Universidade Federal do Rio Grande do Sul. Instituto de Química, Porto Alegre, Brazil, 2009.
48. Demirbas, A. Effects of temperature and particle size on bio-char yield from pyrolysis of agricultural residues. *J. Anal. Appl. Pyrolysis.* **2004**, *72*, 243–248. [CrossRef]
49. Ahalya, N.; Ramachandra, T.V.; Kanamadi, R.D. Biosorption of heavy metals. *Res. J. Chem. Environ.* **2003**, *7*, 71–79.
50. Xie, C.; Xie, Z.; Xu, X.; Yang, D. Persimmon (*Diospyros kaki* L.) leaves: A review on traditional uses, phytochemistry and pharmacological properties. *J. Ethnopharmacol.* **2015**, *163*, 229–240. [CrossRef] [PubMed]
51. Ryu, S.; Furihata, K.; Koda, M.; Wei, F.; Miyakawa, T.; Tanokura, M. NMR-based analysis of the chemical composition of Japanese persimmon aqueous extract. *Magn. Reson. Chem.* **2016**, *54*, 213–221. [CrossRef]
52. Ribeiro, C.M.R.; Souza, N.A. General scheme for elucidating the structure of organic compounds using spectroscopic and spectrometric methods. *Química Nova* **2007**, *30*, 1026–1031. [CrossRef]
53. Ho, Y.S.; Mckay, G. A comparison of chemisorption Kinect models applied to pollutant removal on various sorbents. *Process Saf. Environ. Prot.* **1998**, *76*, 332–340. [CrossRef]
54. Rangabhashiyam, S.; Anu, N.; Giri Nandagopal, M.S.; Selvaraju, N. Relevance of isotherm models in biosorption of pollutants by agricultural byproducts. *J. Environ. Chem. Eng.* **2014**, *2*, 398–414. [CrossRef]
55. Langmuir, I. The constitution and fundamental properties of solids and liquids. *J. Am. Chem. Soc.* **1916**, *38*, 2221–2295. [CrossRef]

56. Langmuir, I. Vapor pressures, evaporation, condensation and adsorption. *J. Am. Chem. Soc.* **1932**, *54*, 2798–2832. [CrossRef]
57. Freundlich, H.M.F. About the adsorption in solution. *Z. Für Phys. Chem.* **1906**, *57*, 385–471.
58. Pearson, G.R. Hard and soft acids and bases. *J. Am. Chem. Soc.* **1963**, *85*, 3533–3539. [CrossRef]
59. Rao, R.A.K.; Ikram, S.; Uddin, M.K. Removal of Cd(II) from aqueous solution by exploring the biosorption characteristics of gaozaban (*Onosma bracteatum*). *J. Environ. Chem. Eng.* **2014**, *2*, 1155–1164.
60. Kumar, B.; Smita, K.; Sánchez, E.; Stael, C.; Cumbal, L. Andean Sacha inchi (*Plukenetia volubilis* L.) shell biomass as new biosorbents for Pb^{2+} and Cu^{2+} ions. *Ecol. Eng.* **2016**, *93*, 152–158. [CrossRef]
61. Martín-Lara, M.A.; Blázquez, G.; Calero, M.; Almendros, A.I.; Ronda, A. Binary biosorption of copper and lead onto pine cone shell in batch reactors and in fixed bed columns. *Int. J. Miner. Process.* **2016**, *148*, 72–82. [CrossRef]
62. Pandey, R.; Prasad, R.L.; Ansari, N.G.; Murthy, R.C. Utilization of NaOH modified *Desmostachya bipinnata* (Kush grass) leaves and *Bambusa arundinacea* (bamboo) leaves for Cd(II) removal from aqueous solution. *J. Environ. Chem. Eng.* **2015**, *3*, 593–602. [CrossRef]
63. Azouaou, N.; Sadaoui, Z.; Djaafri, A.; Mokaddem, H. Adsorption of cadmium from aqueous solution onto untreated coffee grounds: Equilibrium, kinetics and thermodynamics. *J. Hazard. Mater.* **2010**, *184*, 126–134. [CrossRef]
64. Dang, V.B.H.; Doan, H.D.; Dang-vu, T.; Lohi, A. Equilibrium and kinetics of biosorption of cadmium(II) and copper(II) ions by wheat straw. *Bioresour. Technol.* **2009**, *100*, 211–219. [CrossRef]
65. Ghodbane, I.; Nouri, L.; Hamdaoui, O.; Chiha, M. Kinetic and equilibrium study for the sorption of cadmium(II) ions from aqueous phase by eucalyptus bark. *J. Hazard. Mater.* **2008**, *152*, 148–158. [CrossRef] [PubMed]
66. Jain, M.; Garg, V.K.; Kadirvelu, K. Cadmium(II) sorption and desorption in a fixed bed column using sunflower waste carbon calcium–alginate beads. *Bioresour. Technol.* **2013**, *129*, 242–248. [CrossRef] [PubMed]
67. Güzel, F.; Yakut, H.; Topal, G. Determination of kinetic and equilibrium parameters of the batch adsorption of Mn(II), Co(II), Ni(II) and Cu(II) from aqueous solution by black carrot (*Daucus carota* L.) residues. *J. Hazard. Mater.* **2008**, *153*, 1275–1287. [CrossRef] [PubMed]
68. Rahman, M.S.; Islam, M.R. Effects of pH on isotherms modeling for Cu(II) ions adsorption using maple wood sawdust. *Chem. Eng. J.* **2009**, *149*, 273–280. [CrossRef]
69. Chakravarty, P.; Sarma, N.S.; Sarma, H.P. Biosorption of cadmium(II) from aqueous solution using heartwood powder of Areca catechu. *Chem. Eng. J.* **2010**, *162*, 949–955. [CrossRef]
70. Tounsadi, H.; Khalidi, A.; Abdennouri, M.; Barka, N. Biosorption potential of Diplotaxis harra and Glebionis coronaria L. biomasses for the removal of Cd(II) and Co(II) from aqueous solutions. *J. Environ. Chem. Eng.* **2015**, *3*, 822–830. [CrossRef]
71. Coelho, G.F.; Gonçalves, A.C., Jr.; Tarley, C.R.T.; Casarin, J.; Nacke, H.; Francziskowski, M.A. Removal of metal ions Cd (II), Pb (II), and Cr (III) from water by the cashew nut shell *Anacardium occidentale* L. *Ecol. Eng.* **2014**, *73*, 514–525. [CrossRef]
72. Moyo, M.; Guyo, U.; Mawenyiyo, G.; Zinyama, M.P.; Nyamunda, B.C. Marula seed husk (*Sclerocarya birrea*) biomass as a low cost biosorbent for removal of Pb(II) and Cu(II) from aqueous solution. *J. Ind. Eng. Chem.* **2015**, *27*, 126–132. [CrossRef]
73. Liu, C.; Ngo, H.H.; Guo, W.; Tung, K.L. Optimal conditions for preparation of banana peels, sugarcane bagasse and watermelon rind in removing copper from water. *Bioresour. Technol.* **2012**, *119*, 349–354. [CrossRef]
74. Aydin, H.; Bulut, Y.; Yerlikaya, Ç. Removal of copper (II) from aqueous solution by adsorption onto low-cost adsorbents. *J. Environ. Manag.* **2008**, *87*, 37–45. [CrossRef]
75. Rao, R.A.K.; Ikram, S. Sorption studies of Cu(II) on gooseberry fruit (*Emblica officinalis*) and its removal from electroplating wastewater. *Desalination* **2011**, *277*, 390–398. [CrossRef]
76. Lasheen, M.R.; Ammar, N.S.; Ibrahim, H.S. Adsorption/desorption of Cd(II), Cu(II) and Pb(II) using chemically modified orange peel: Equilibrium and kinetic studies. *Solid State Sci.* **2012**, *14*, 202–210. [CrossRef]
77. Ahmad, R.; Haseeb, S. Absorptive removal of Pb^{2+}, Cu^{2+} and Ni^{2+} from the aqueous solution by using groundnut husk modified with Guar Gum (GG): Kinetic and thermodynamic studies. *Groundw. Sustain. Dev.* **2015**, *1*, 41–49. [CrossRef]
78. Ding, Y.; Jing, D.; Gong, H.; Zhou, L.; Yang, X. Biosorption of aquatic cadmium(II) by unmodified rice straw. *Bioresour. Technol.* **2012**, *114*, 20–25. [CrossRef] [PubMed]
79. Alslaibi, T.M.; Abustan, I.; Ahmad, M.A.; Foul, A.A. Cadmium removal from aqueous solution using microwaved olive stone activated carbon. *J. Environ. Chem. Eng.* **2013**, *1*, 589–599. [CrossRef]
80. Dong, J.; Hu, J.; Wang, J. Radiation-induced grafting of sweet sorghum stalk for copper(II) removal from aqueous solution. *J. Hazard. Mater.* **2013**, *262*, 845–852. [CrossRef]
81. Wang, F.Y.; Wang, H.; Ma, J.W. Adsorption of cadmium (II) ions from aqueous solution by a new low-cost adsorbent—Bamboo charcoal. *J. Hazard. Mater.* **2010**, *177*, 300–306. [CrossRef]

Disclaimer/Publisher's Note: The statements, opinions and data contained in all publications are solely those of the individual author(s) and contributor(s) and not of MDPI and/or the editor(s). MDPI and/or the editor(s) disclaim responsibility for any injury to people or property resulting from any ideas, methods, instructions or products referred to in the content.